Geophysical Research Letters

RESEARCH LETTER
10.1029/2019GL086437

The Tropical Atmospheric Conveyor Belt: A Coupled Eulerian-Lagrangian Analysis of the Large-Scale Tropical Circulation

Dana Raiter[1], **Eli Galanti**[1], **and Yohai Kaspi**[1]

[1]Department of Earth and Planetary Sciences, Weizmann Institute of Science, Rehovot, Israel

Key Points:
- An Eulerian analysis reveals that the atmospheric meridional circulation in the tropics has a strong longitudinal dependence
- A Lagrangian analysis reveals that the actual movement of air in the tropical atmosphere is affected by all components of the 3-D flow
- The actual circulation in the tropics can be described as an atmospheric conveyor belt, with the Indo-Pacific convection being its driver

Supporting Information:
- Supporting Information S1

Correspondence to:
D. Raiter,
dana.raiter@weizmann.ac.il

Citation:
Raiter, D., Galanti, E., & Kaspi, Y. (2020). The tropical atmospheric conveyor belt: A coupled Eulerian-Lagrangian analysis of the large-scale tropical circulation. *Geophysical Research Letters*, *47*, e2019GL086437. https://doi.org/10.1029/2019GL086437

Received 28 NOV 2019
Accepted 26 MAR 2020
Accepted article online 28 MAR 2020

Abstract The Hadley circulation is a key element of the climate system. It is traditionally defined as the zonally averaged meridional circulation in the tropics, therefore treated as a zonally symmetric phenomenon. However, differences in temperature between land and sea cause zonal asymmetries on Earth, dramatically affecting the circulation. This longitudinal dependence of the meridional circulation evokes questions about where and when the actual large-scale tropical circulation occurs. Here, we look into the connection between the longitudinally dependent meridional circulation, and the actual large-scale transport of air in the tropics using a coupled Eulerian and Lagrangian approach. Decomposing the velocity field into rotational and divergent components, we identify how each component affects the actual circulation. We propose an alternative definition for the circulation, which describes the actual path of air parcels in the tropics, as a tropical atmospheric conveyor belt.

Plain Language Summary The large-scale circulation of air in the tropics is traditionally represented by a closed north-south cell averaged over all longitudes (the Hadley circulation). However, differences in temperature between land and sea cause significant variations in the circulation at different longitudes. The variations evoke questions about where and when the actual large-scale tropical circulation occurs. In this study, we combine two approaches, the first, looking at the local components of the flow, and the second, tracking air parcels following their path in the atmosphere. The combined analysis reveals the actual flow pattern that can be described as a conveyor belt, circulating the air in the tropics. The Indo-Pacific region is the engine of this circulation, where air converges and ascends, then moves westward and southward (northward) in July (January), merges into the jet stream at approximately 25°S (25°N) and moves rapidly to the east, eventually descending near the Americas.

1. Introduction

The Hadley circulation (HC) is responsible for the majority of the heat transport in the tropics and is strongly tied to many phenomena including the trade winds, the subtropical deserts, and the subtropical jet streams (Hartmann, 2016). The importance of the HC stimulated countless studies on the mechanisms controlling the circulation and its temporal variability (e.g., Dima & Wallace, 2002; Held & Hou, 1980; Lindzen & Hou, 1988). The HC is traditionally defined as the zonally averaged meridional circulation (Vallis, 2017), overlooking the zonal asymmetry on Earth, and therefore creating a two dimensional perception of the circulation. The traditional definition has proven very useful for understanding the phenomenon and its variability. Many studies have been conducted about the variability of the zonally averaged meridional circulation in past and present times, as well as for the future, under climate change (e.g., Chemke & Polvani, 2019; Diaz & Bradley, 2004). Others used the traditional definition for theoretical understanding of the HC. For example, Held and Hou (1980) introduced a theory that explains the width of the HC making several assumptions, including zonal symmetry. However, differences in temperature between land and sea cause variability in observations at different longitudes, leading to a more complex structure of the HC in reality. This led to a more local analysis of regional and seasonal aspects of the HC, by analyzing, for example, the vertical and meridional velocities as function of latitude and longitude, and trajectories of the climatological flow emphasizing the regional aspects of the HC (Karnauskas & Ummenhofer, 2014).

A different approach is to decompose the velocity field into rotational and divergent components (Helmholtz decomposition), and then by using only the divergent component of the flow, the localized meridional

circulation can be calculated (Keyser et al., 1989). Schwendike et al. (2014) used this decomposition method to calculate the relative contributions of the vertical mass fluxes in the middle troposphere to the Hadley and Walker circulations. The same method was also used to study specific regions of interest, such as the Atlantic sector of the HC during the boreal summer and its connection to the Atlantic tropical cyclone activity (Zhang & Wang, 2013), and the variability of the HC in the Southern Hemisphere in different sectors of the world (Nguyen et al., 2018). The same methodology was used to study the interdecadal trend of both the Hadley and Walker circulations, where it was shown that in order to understand the effect of climate variability on the tropical circulation patterns, the analysis should be regional (Schwendike et al., 2015). In a following study, Staten et al. (2019) analyzed the regional expansion of the HC under climate change.

The decomposition into the divergent and rotational components is very useful for understanding the longitudinal variations of the meridional circulation, helping to locate where the circulation occurs. However, analyzing one component of the circulation gives an incomplete picture that does not represent the actual flow. The velocity field is constructed from all components, and therefore it is necessary to understand the effect of each component on the flow. Moreover, even when analyzing all components, it is impossible to obtain the actual movement of the air in the atmosphere using this Eulerian approach, since the combined effect of all components is not apparent when observing each component separately. Therefore, an analysis of the actual movement of air is required, one that captures and visualizes the contribution of all the components together.

Here, we investigate the longitudinally dependent large-scale tropical circulation using a coupled Eulerian and Lagrangian approach. Taking the Eulerian approach of using the Helmholtz decomposition method, calculating the climatological meridional circulation at each longitude, combined with the Lagrangian approach of tracking air parcels in the atmosphere, allows to understand the actual movement of air associated with the large-scale tropical circulation. This combined approach enables the development of a complete and global picture of the large-scale tropical circulation.

2. Decomposition of the Velocity Field: Eulerian Approach

Using the Helmholtz decomposition (e.g., Hu et al., 2017; Keyser et al., 1989; Schwendike et al., 2014), the observed velocity field can be decomposed into rotational and divergent components. Following the notation of Hu et al. (2017), the horizontal divergence of the wind is

$$D = \nabla \cdot \mathbf{v}, \tag{1}$$

where $\mathbf{v} = (u, v)$ is the horizontal wind vector, with u and v being the zonal and meridional components, respectively, and the divergence is taken on constant pressure surfaces. Then, a potential function χ is calculated via

$$\nabla^2 \chi = D. \tag{2}$$

This potential represents only the divergent part of the horizontal flow, and therefore, it can be used to calculate the divergent wind

$$\nabla \chi = \mathbf{v}_{\text{div}}, \tag{3}$$

where $\mathbf{v}_{\text{div}} = \left(u_{\text{div}}, v_{\text{div}}\right)$. This velocity field satisfies the continuity equation: $\nabla \cdot \mathbf{v}_{\text{div}} + \frac{\partial \omega}{\partial p} = 0$. Finally, the divergent wind can be used to calculate the longitudinally dependent meridional circulation

$$\psi(\phi, \theta, p, t) = \frac{1}{g} \int_0^p v_{\text{div}}(\phi, \theta, p', t) dp', \tag{4}$$

where ϕ, θ, p, and t are the longitude, latitude, pressure, and time, respectively, and g is the gravitational acceleration. Similarly, using u_{div} (u_{rot}) the zonal (rotational) circulation can be calculated (see supporting information).

In this study, we use the European Center for Medium Range Weather Forecasts ERA-Interim reanalysis data covering the years 1979–2018 (Dee et al., 2013). First, from the latitudinally dependent meridional circulation, ψ (equation (4)), we reproduce the classic double Hadley cells by calculating its zonal and time

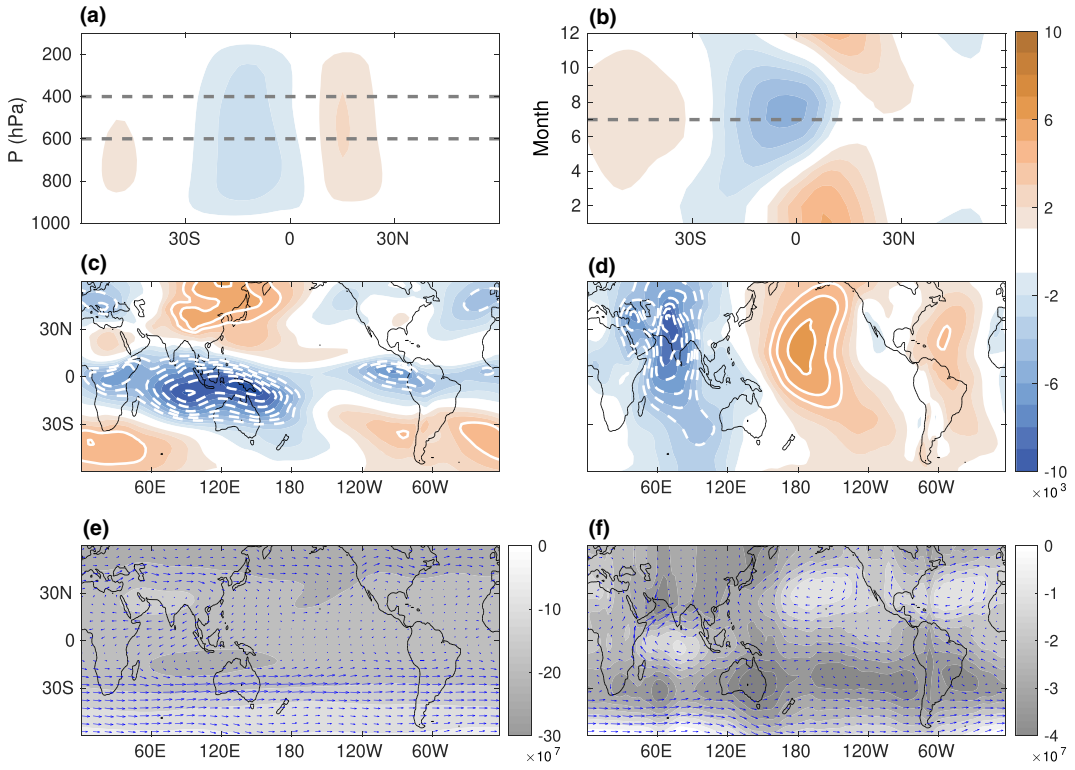

Figure 1. (a) The annually and zonally averaged meridional circulation as function of latitude and pressure, with the dashed lines denoting the 400 and 600 hPa levels. (b) The zonal mean meridional circulation, averaged between 400 and 600 hPa, as function of latitude and month of the year, with the dashed line denoting July. (c–f) The time average of the different components of the circulation in July as function of longitude and latitude. (c) The meridional circulation and (d) the zonal circulation, both averaged between 400 and 600 hPa. (e) The rotational circulation at 200 hPa and (f) the rotational circulation at 850 hPa. Arrows indicate the rotational component of the horizontal velocity. (a–d) Contour interval is 1×10^3 kg s^{-1} m^{-1}, and white solid and dashed lines indicate absolute values larger than 4×10^3 kg s^{-1} m^{-1}. (e, f) Colored contours are in units of m^2 s^{-1}. Note that the traditional mass stream function, given in kg s^{-1} can be obtained by multiplying (a–c) by a factor of $2\pi a \cos\theta$.

average over all years (Figure 1a). The circulation is found to be most intense between 400 and 600 hPa. Averaging ψ between 400 and 600 hPa, and presenting the circulation as function of latitude and month of the year (Figure 1b), the well-known seasonal cycle emerges, reaching maximum values in January (Northern Hemisphere (NH) winter) and July (Southern Hemisphere (SH) winter). The climatology of the longitudinally dependent circulation in July is obtained by averaging ψ between 400 and 600 hPa as well as time averaging over all the July months between 1979-2018 (Figure 1c). In this description air is rising and descending in the white areas. The ascending (descending) branch goes north (south) for orange contours and south (north) for blue contours. The variability in longitude is very prominent (Figure 1c) with a strong cell between 50°E and 150°W. Between 160°W and 60°W there is a much smaller and far weaker cell. In other words, the circulation in the tropics is, in fact, not zonally symmetric prompting the need to take into account its longitudinal dependence.

Following the same steps, we calculate, using u_{div}, the latitudinally dependent zonal (Walker) circulation (Figure 1d), and the rotational circulation using u_{rot} at 200 and 850 hPa (Figures 1e and 1f). It is apparent that all circulations have strong spatial variations, and each component affects the actual motion of air in the atmosphere. For example, the strong ascent in the West Pacific participates in both the meridional and zonal circulations there. The rotational components contribute to the movement only in the horizontal direction, which will not be captured when examining only the meridional circulation. Thus, in order to understand what dominates the movement of air in the tropical atmosphere, we need to analyze the magnitude and direction of each component and its contribution to the overall circulation. Note that a similar analysis for January is presented in the supporting information (Figure S1).

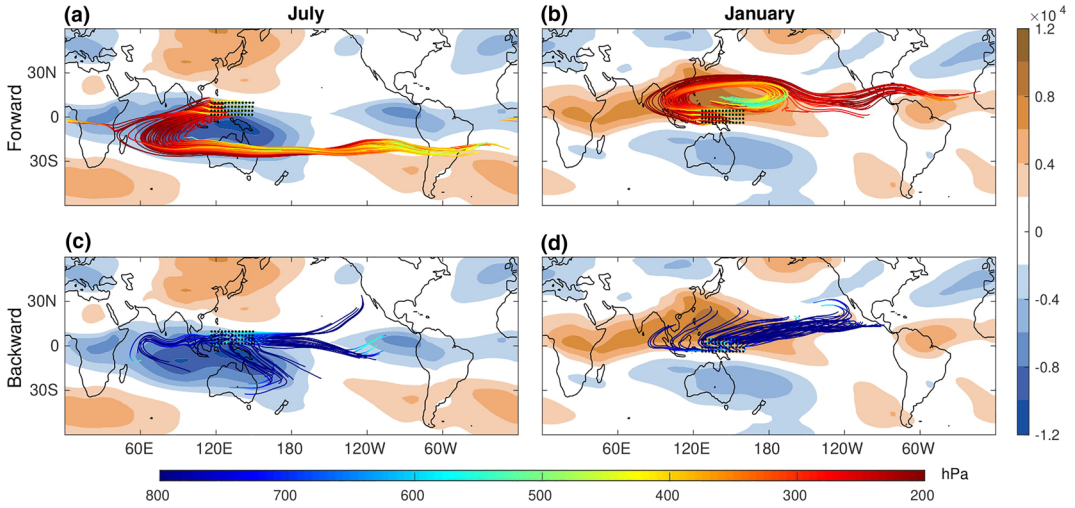

Figure 2. Mean flow trajectories and meridional circulation for July (left) and January (right). Shown is the meridional circulation at 500 hPa (contours), with contour interval of 2×10^3 kg s^{-1} m^{-1}. The lines show the air parcels trajectories going 20 days forward (a, b) and 20 days backward (c, d) in time. The initial locations are marked with black dots. The color of the lines indicates the pressure level in hPa (bottom color bar).

3. The Movement of Air in the Tropics: Lagrangian Approach

The Eulerian analysis, exposing the distinct spatial patterns of the circulation, prompts several questions: what does the real movement of air in the tropics look like, and how is it connected to the patterns? What is the typical time scale of this motion and is the air involved in the circulation confined to the tropics? To answer these questions, we use LAGRANTO (Sprenger & Wernli, 2015), a Lagrangian analysis tool that calculates trajectories of air parcels (see supporting information). Using the climatological flow for July and January we calculate representative trajectories for each month (Figure 2). In each of them, we follow a total of 52 trajectories for 20 days. The initial locations of air parcels are selected where there is a strong ascent near the equator at a height of 500 hPa (black dots), corresponding to the strongest north-south shear in the dominant meridional overturning circulation. This ascent is also evident in the vertical velocity (see supporting information). In the next analysis we discuss trajectories of air parcels with different initial positions and further demonstrate why the Indo-Pacific is the main area of interest (Figure 3).

The meridional circulation is easily identified in both months (Figure 2), with the air rising locally near the equator, moving south in July and north in January and then descending. However, in addition to this movement there is a strong movement in the east-west direction. Hence, the 3-D movement of the air parcels needs to be described taking into account all the different components of the velocity field (Figures 1c–1f), in addition to the longitudinally dependent meridional circulation. It appears that in July, air parcels ascend mostly locally, move west due to the rotational component of the horizontal velocity, and then move south due to the meridional circulation (Figure 2a). When the air parcels reach approximately 25°S, they merge into the jet stream (at its equatorial side) and move eastward rapidly, eventually descending near the Americas. In January, the picture is somewhat more elaborate because of the more complex continental configuration in the NH (Figure 2b). However, the main path is still visible, with air rising locally and moving slightly west and then to the north. When the air parcels reach the jet stream, approximately half of them move eastward with the jet and stay at high altitudes even after 20 days. The other half of the air parcels, which reach the southern boundary of the jet stream, start to descend and veer west with the trade winds (see supporting information for details).

In order to complete the analysis of the circulation, we calculate also the back trajectories for January and July, starting from the same initial positions (Figures 2c and 2d). The movement of air parcels takes place mostly at lower altitudes; therefore, the movement is slower. In both July and January, easterlies generate convergence of air parcels from the East Pacific to the starting positions. In July the air parcels appear to converge from the West Pacific as well, moving with the Walker circulation and with the rotational component of the horizontal wind at low altitudes.

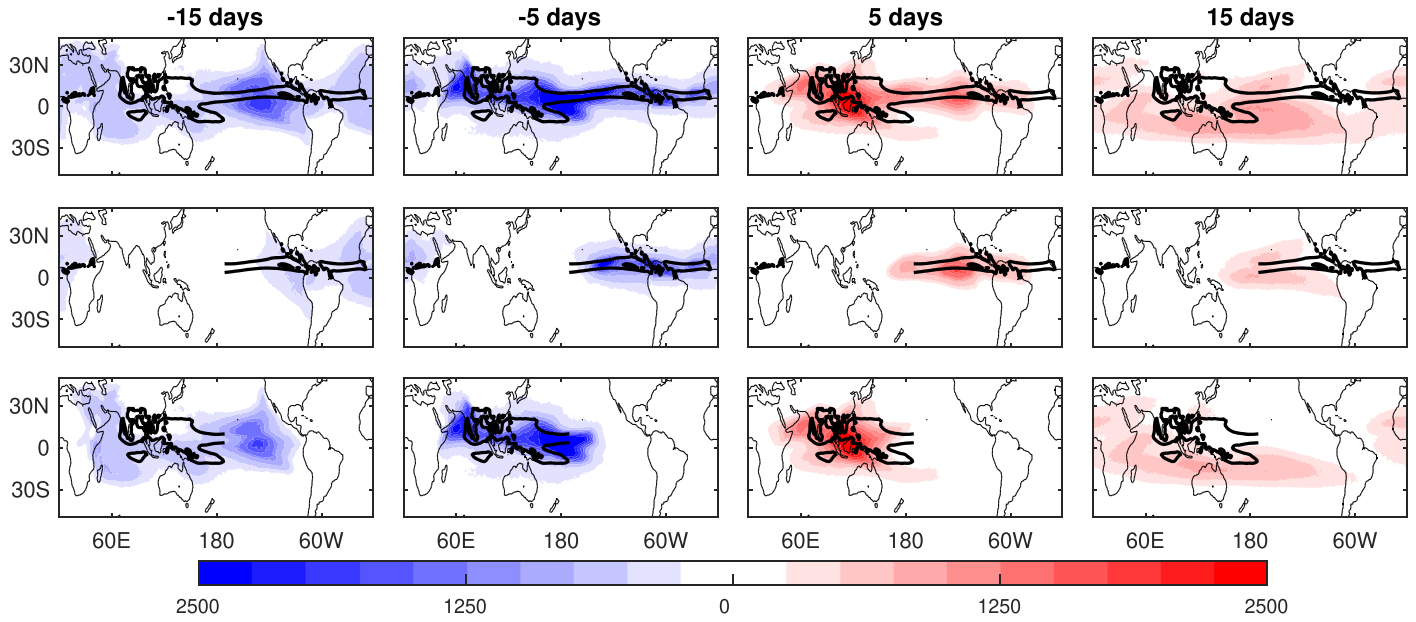

Figure 3. Distribution of air parcels in different sectors for all July months during 1979–2018. The black contour marks air parcels' initial position at 500 hPa, and the density of air parcels (number of parcels per a 1° × 1° grid box) is marked in red for forward trajectories and blue for backward trajectories. The top row shows the density of all tracked air parcels, the middle row shows parcels initially located in the East Pacific and Atlantic Oceans, and the bottom row shows parcels initially located in the Indo-Pacific. Shading indicates the relative number of air parcels at the specific location and time.

The trajectories of the climatological flow, while useful for understanding the dominating path of air parcels, do not accurately represent the movement of air in reality, because the flow field is averaged in time, and variability and localized movement is lost. To address this issue, we calculate the trajectories of air parcels without averaging over time, maintaining the variability. In order to visualize these trajectories, we calculate their spatial density. First, we define the region of initial positions of air parcels, by selecting a region of high rainfall, with more than 6 mm day^{-1} in the climatological convective precipitation (Figure 3, black contour in upper panels). This region exhibits strong convection, associated with the ascending branch of the meridional circulation. We then calculate the trajectories of air parcels initially positioned in this region, using the 6-hourly data from Era-Interim for every July from 1979 to 2018. In total, we follow over 2,000 starting positions and 4,800 starting times, resulting in millions of air parcels. Next, we mark each air parcel's position every 6 hrs, creating a distribution plot of all parcels without averaging over time.

Figure 3 shows the distribution of air parcels at −15, −5, 5, and 15 days relative to the time of initiation of the parcels in July. The top panels show all air parcels initially positioned at the high convection zone. The main path of air parcels visualized above (Figures 2a and 2b) is clearly visible here. Air parcels move westward after 5 days, and after 15 days the movement south and eastward becomes prominent. In order to further clarify the movement of the air parcels, we separate the starting locations into two regions. The middle and bottom panels of Figure 3 show air parcels initially positioned in the East Pacific and Atlantic Ocean, and in the Indo-Pacific region, respectively. The East Pacific and Atlantic air parcels show a rather confined movement, corresponding to the smaller and weaker overturning cell exhibited in the longitudinally dependent meridional circulation at the same location (Figure 1c). The Indo-Pacific air parcels (bottom panels), on the other hand, participate in the circulation as it is defined with strong movement to the west, and later to the south and to the east. Hence, the Indo-Pacific region acts as the engine of the large-scale tropical circulation.

Distribution of back trajectories (Figure 3, left panels) explains where the air parcels that participate in the circulation come from. In the East Pacific and Atlantic region (middle row) we see localized movement yet again, since these air parcels do not participate in the circulation. The air parcels converging into the Indo-Pacific region (bottom), however, reveal a few interesting features. First, as expected, air parcels converge into the Indo-Pacific from the East Pacific with the trade winds. Second, air parcels come also from the Indian Ocean, moving east. Third, while it would be expected that air parcels return mostly from the south, where they reach after 15 days, there is a symmetry between the NH and the SH; that is, air parcels from both hemispheres converge into the Indo-Pacific. Although a closure of the circulation

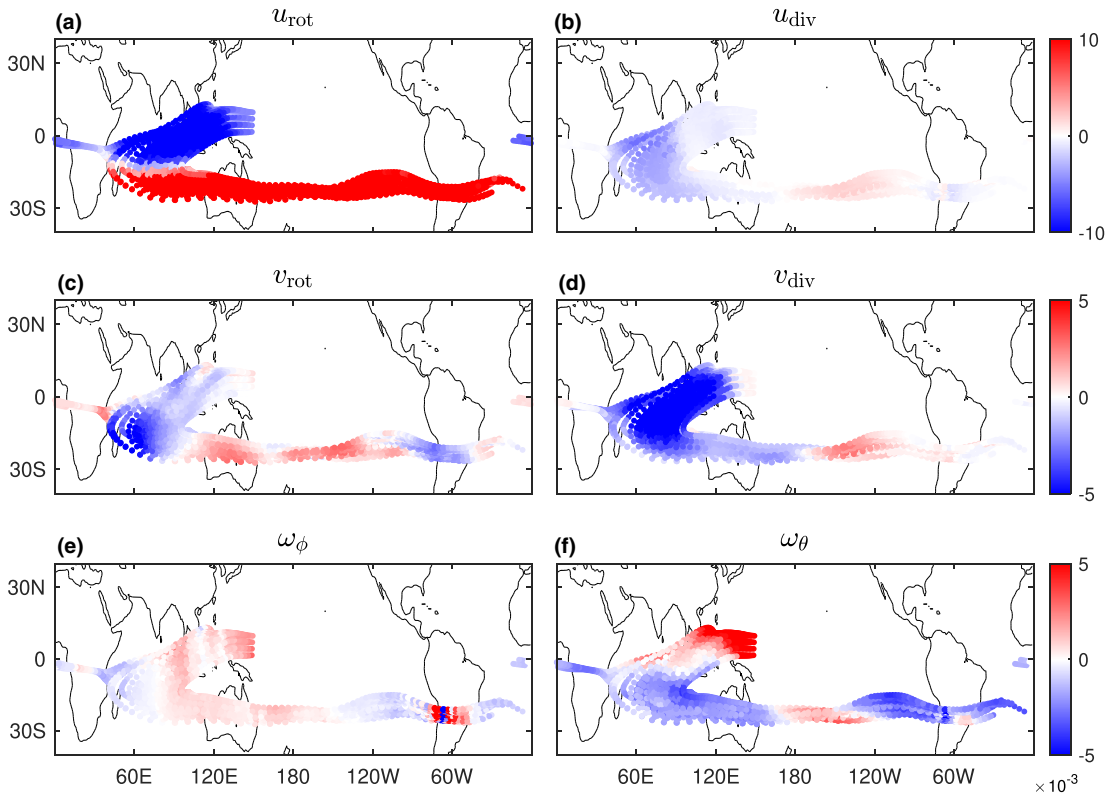

Figure 4. Contribution of each component of the decomposed velocity field to the mean flow movement in July, at the locations of the air parcels shown in Figure 2. Color indicates the magnitude of the velocity component in m s^{-1} (Pa s^{-1}) for the horizontal (vertical) wind; (u_{rot}, v_{rot}) and (u_{div}, v_{div}) are the rotational and divergent components of the horizontal wind, respectively; u_{div} participates only in the zonal circulation, and v_{div} participates only in the meridional circulation; ω_ϕ is the component of the vertical velocity that participates in the zonal circulation, and ω_θ is the component of the vertical velocity that participates in the meridional circulation.

is not entirely apparent, it seems that 30 days is approximately the typical time scale of the circulation, since during this span, air parcels converge and diverge. Lastly, the air parcels are confined between approximately 30°S and 30°N, the limits of the traditionally defined HC. A similar analysis for January (Figure S3 in the supporting information) shows that the behavior of air parcels is similar to July (in the corresponding winter hemisphere), and once again the Indo-Pacific region appears to be the driver of the circulation.

The fact that the main features of the mean flow climatological trajectories (Figure 2) are exhibited in the density of the 40 years hourly trajectories reassures the use of the mean flow trajectories as a representation of the main path of air parcels. To further clarify the contribution of each component of the velocity field to the actual movement of air, we plot the contribution from the different velocity components at the locations of the air parcels in the mean flow trajectories in July (Figure 4). Note that the locations are a function of height (pressure), in addition to the latitude-longitude location. The horizontal wind is decomposed using equation (1)–(3), while the decomposition of the vertical velocity is calculated following the notation of Schwendike et al. (2014) (see supporting information).

The rotational component of the zonal flow (u_{rot}) is the strongest of all the components (Figure 4a), dominating the easterlies near the equator and the jet stream at approximately 25°S. The contribution of the divergent component of the zonal wind (u_{div}), which participates in the zonal circulation is relatively small (Figure 4b); therefore, both for the initial westward motion and for the eastward motion along the jet stream, the dominating path of air parcels is almost entirely due to the rotational zonal wind. The meridional wind, on the other hand, shows a very different behavior (Figures 4c and 4d). The divergent component of the meridional velocity (v_{div}) dominates the movement to the south after the initial ascent near the equator. The rotational component of the meridional wind (v_{rot}) is much weaker than the divergent component in the same region, with some contribution at the most western part of the southward movement. Along the jet

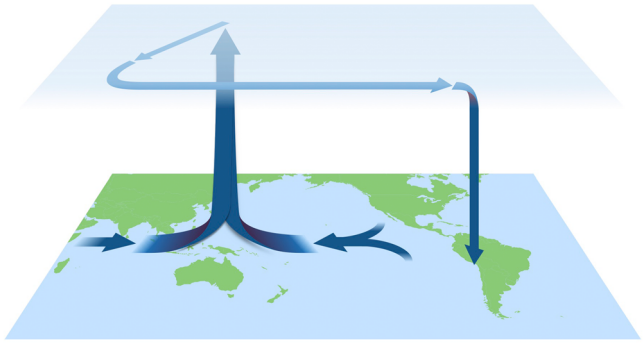

Figure 5. A schematic of the dominant path of air parcels participating in the large-scale tropical conveyor for July. The air parcels converge into the Indo-Pacific, ascend, move to the west and to the south, merge into the jet stream, and move east, eventually descending near the Americas.

stream the flow oscillates latitudinally, with similar significance to both v_{rot} and v_{div}. Note that the variations in v_{div} show the longitudinal dependence of the meridional circulation. Lastly, The component of the vertical wind (Figures 4e and 4f) that participates in the meridional circulation (ω_θ) is much more dominant than the component that participates in the zonal circulation (ω_ϕ), in accordance with the regional Walker circulation being weaker than the regional HC (Schwendike et al., 2014).

As expected, at the initial position of the air parcels (Figure 2, black dots), there is contribution from both components to the ascending motion that generates a stronger upward motion. Interestingly, the meridional circulation, ω_θ, dominates the downward motion at 25°S, with a moderate contribution at 120°E to 180°, and a stronger region at 120–60°W, and it also exhibits mild upward wind at 180° to 120°W. Therefore, it is apparent that the decent of the air is dominated by the meridional circulation, with most of it happening close to the Americas and some in the Australian region (this is also apparent in Figure 2a). Still, even in regions of weak meridional circulation, there is descent of air in the subtropics, resulting in the existence of subtropical deserts far from the regions of the strongest circulation.

In January (Figure S4 in the supporting information), the components of the velocity field feature similar relationships between each other as in July. However, one notable difference is the significance of v_{rot} with respect to v_{div}. In January, the magnitude of v_{rot} in some regions is as dominant as, or even more dominant than, v_{div}, which explains the veering of half of the trajectories southward (Figure 2b).

4. Discussion and Summary

The large-scale circulation in the tropics is traditionally described in terms of the HC, a definition that does not take into account variability with longitude. In the past decade, studies have shown that the circulation strongly depends on the longitudinal position (e.g., Karnauskas & Ummenhofer, 2014; Nguyen et al., 2018; Schwendike et al., 2014), raising the question of how does the air actually circulate in the tropics. In this study, we revisit this question by using a combination of Eulerian and Lagrangian analyses.

Decomposing the velocity field into rotational and divergent components, we analyze the longitudinal dependence of the tropical circulation. The strong variations in longitude (Figure 1) motivate inspection of the actual movement of air in the tropical atmosphere, that is, to analyze the velocity field with a Lagrangian approach. Calculating trajectories of the mean flow reveals a complex pattern, involving all components of the velocity field (Figure 2). This pattern is also exhibited in the density of trajectories (Figure 3). Looking at the distribution of the air parcels, it is noticeable that the circulation is indeed regional, where the Indo-Pacific region is the driver of the circulation. Furthermore, we find that all components of the decomposed velocity field contribute significantly to the circulation.

Combining the Eulerian and Lagrangian approaches, we are able to analyze the circulation in the tropics considering all aspects of the circulation, without any presumptions. The Eulerian analysis gives information about the different types of circulations (rotational, meridional and zonal) isolated from one another, making it easy to understand the contribution of each component to the entire circulation. The Lagrangian analysis, on the other hand, compiles all components to a 3-D pattern of the circulation, where the effect of each component is visible in the air parcels' paths. Hence, although it is useful to decompose the circulation into different components, in reality, all components are required to explain the motion of air. This is further established when exploring the contribution of the different components of the velocity field at the locations of air parcels in the mean flow trajectories (Figure 4).

The combined Eulerian-Lagrangian analysis, which takes into account all the components of the velocity field, reveals a circulation pattern in the tropics that can be described as a conveyor belt (Figure 5). Air converges into the Indo-Pacific Warm Pool, which acts as the engine of the circulation. This air ascends, moves westward in the upper levels with the rotational winds, and then poleward with the meridional circulation. It reaches approximately 25°S (or 25°N in the opposite season), merges into the jet stream and moves

rapidly to the east. Finally, it descends near the Americas. This new definition more accurately represents the circulation in the tropics and shows the regionality and three-dimensionality of the circulation as manifested in the Eulerian and Lagrangian analyses.

Acknowledgments
This research has been supported by the Israeli Science Foundation (Grant 1819/16). ECMWF Era-Interim reanalysis data (Dee et al., 2013) can be downloaded online (https://www.ecmwf.int/en/forecasts/datasets/reanalysis-datasets/era-interim).

References

Chemke, R., & Polvani, L. M. (2019). Exploiting the abrupt 4×CO2 scenario to elucidate tropical expansion mechanisms. *Journal of Climate*, *32*(3), 859–875. https://doi.org/10.1175/JCLI-D-18-0330.1

Dee, D. P., Uppala, S., Simmons, A., Berrisford, P., Poli, P., Kobayashi, S., et al. (2013). The ERA-Interim reanalysis: Configuration and performance of the data assimilation system. *Quarterly Journal of the Royal Meteorological Society*, *137*(656), 553–597. https://doi.org/10.1002/qj.828

Diaz, H. F., & Bradley, R. S. (2004). The Hadley circulation: Present, past, and future. *The Hadley circulation: Present, past and future* (pp. 1–5). Dordrecht: Springer Netherlands. https://doi.org/10.1007/978-1-4020-2944-8

Dima, I. M., & Wallace, J. M. (2002). Notes and correspondence on the seasonality of the Hadley cell. *Journal of the Atmospheric Sciences*, *60*, 1522–1527. https://doi.org/10.1175/1520-0469(2003)060<1522:OTSOTH>2.0.CO;2

Hartmann, D. L. (2016). Chapter 6-Atmospheric general circulation and climate. *Global physical climatology (second edition)* (2nd ed., pp. 159–193). Boston: Elsevier.

Held, I. M., & Hou, A. Y. (1980). Nonlinear axially symmetric circulations in a nearly inviscid atmosphere. *Journal of the Atmospheric Sciences*, *37*, 515–533. https://doi.org/10.1175/1520-0469(1980)037<0515:NASCIA>2.0.CO;2

Hu, S., Cheng, J., & Chou, J. (2017). Novel three-pattern decomposition of global atmospheric circulation: Generalization of traditional two-dimensional decomposition. *Climate Dynamics*, *49*(9-10), 3573–3586. https://doi.org/10.1007/s00382-017-3530-3

Karnauskas, K. B., & Ummenhofer, C. C. (2014). On the dynamics of the Hadley circulation and subtropical drying. *Climate Dynamics*, *42*(9), 2259–2269. https://doi.org/10.1007/s00382-014-2129-1

Keyser, D., Schmidt, B. D., & Duffy, D. G. (1989). A technique for representing three-dimensional vertical circulations in baroclinic disturbances. *Monthly Weather Review*, *117*(11), 2463–2494. https://doi.org/10.1175/1520-0493(1989)117<2463:ATFRTD>2.0.CO;2

Lindzen, R. S., & Hou, A. V. (1988). Hadley circulations for zonally averaged heating centered off the equator. *Journal of the Atmospheric Sciences*, *45*(17), 2416–2427. https://doi.org/10.1175/1520-0469(1988)045<2416:HCFZAH>2.0.CO;2

Nguyen, H., Hendon, H. H., Lim, E. P., Boschat, G., Maloney, E., & Timbal, B. (2018). Variability of the extent of the Hadley circulation in the southern hemisphere: A regional perspective. *Climate Dynamics*, *50*(1), 129–142. https://doi.org/10.1007/s00382-017-3592-2

Schwendike, J., Berry, G. J., Reeder, M. J., Jakob, C., Govekar, P., & Wardle, R. (2015). Trends in the local Hadley and local Walker circulations. *Journal of Geophysical Research: Atmospheres*, *120*, 7599–7618. https://doi.org/10.1002/2014JD022652

Schwendike, J., Govekar, P., Reeder, M. J., Wardle, R., Berry, G. J., & Jakob, C. (2014). Local partitioning of the overturning circulation in the tropics and the connection to the Hadley and Walker circulations. *Journal of Geophysical Research: Atmospheres*, *119*, 1322–1339. https://doi.org/10.1002/2013JD02074

Sprenger, M., & Wernli, H. (2015). The LAGRANTO lagrangian analysis tool version 2.0. *Geoscientific Model Development*, *8*(8), 2569–2586. https://doi.org/10.5194/gmd-8-2569-2015

Staten, P. W., Grise, K. M., Davis, S. M., Karnauskas, K., & Davis, N. (2019). Regional widening of tropical overturning: Forced change, natural variability, and recent trends. *Journal of Geophysical Research: Atmospheres*, *124*, 6104–6119. https://doi.org/10.1029/2018JD030100

Vallis, G. K. (2017). *Atmospheric and oceanic fluid dynamics: Fundamentals and large-scale circulation* (2nd ed., 946 pp.). Cambridge University Press.

Zhang, G., & Wang, Z. (2013). Interannual variability of the Atlantic Hadley circulation in boreal summer and its impacts on tropical cyclone activity. *Journal of Climate*, *26*(21), 8529–8544. https://doi.org/10.1175/JCLI-D-12-00802.1